



COVER SHEET

This is the author version of article published as:

Frost, Ray L. and Wills, Rachael-Anne and Weier, Matt L. and Martens, Wayde N. (2005) A comparison of the Raman spectra of natural and synthetic K and Na-jarosites at 298 and 77 K. *Journal of Raman Spectroscopy* 36(5):pp. 435-444.

Copyright 2005 John Wiley & Sons

Accessed from <http://eprints.qut.edu.au>

A comparison of the Raman spectra of natural and synthetic K and Na-jarosites at 298 and 77 K

Ray L. Frost*, Matt L. Weier and Wayde Martens

Inorganic Materials Research Program, School of Physical and Chemical Sciences, Queensland University of Technology, GPO Box 2434, Brisbane Queensland 4001, Australia.

Abstract

Raman spectroscopy at 298 and 77 K has been used to characterise synthetic and natural jarosites of formula $M_n(\text{Fe}^{3+})_6(\text{SO}_4)_4(\text{OH})_{12}$ where M is K or Na. The natural jarosites are characterised by a well define hydroxyl stretching pattern in contrast to that of the synthetic jarosites. This difference is attributed to differences in hydrogen bonding in the mineral. Multiple Raman OH stretching bands are indicative of non-equivalent OH units in the structure. Jarosites are characterised by an intense sharp band between 1007 and 1010 cm^{-1} attributed to the sulphate symmetric stretching mode. The band width for K-jarosite is 4.4 cm^{-1} at 298 K and 3.6 cm^{-1} at 77 K in comparison to the values for synthetic jarosite of 10.0 (298 K) and 7.3 cm^{-1} (77 K). Differences in the spectra between the natural and synthetic jarosites are found. Reasons for these differences in the spectra are provided.

Introduction

Interest in the chemistry of jarosites stems from a number of reasons. Firstly because of the discovery of jarosites on Mars^{1,2}. Such a find implies the presence of water on Mars either at present or at some time in the planetary past^{3,4}. Interest in such minerals and their thermal stability rests with the possible identification of these minerals and related dehydrated paragenetically related mineral on planets and on Mars. There have been many studies on related minerals such as the Fe(II) and Fe(III) sulphate minerals⁵⁻¹⁰. Secondly jarosites are found in soils and evaporate deposits. The importance of jarosite formation and its decomposition depends upon its presence in soils, sediments and evaporate deposits¹¹. These types of deposits have formed in acid soils where the pH is less than 3.0 pH units¹². Such acidification results from the oxidation of pyrite which may be from bacterial action or through air-oxidation. Thirdly jarosites are important from an environmental point of view. Jarosites are minerals which can function as collectors of heavy metals and low concentrations can be found in the natural jarosites. Such minerals can act as a significant environmental sink¹³. Jarosites may be useful for the uptake of Ce^{6+} and As^{5+} in ground waters¹⁴. Such an application remains to be explored.

One of the difficulties associated with the analysis of jarosites is that they are often poorly crystalline, making detection using XRD techniques difficult. Another problem associated with the study of jarosites is their thermodynamic stability¹⁵. Often the minerals are formed from acid-sulfate rich environments such as acid mine drainage and acid-sulfate soils and as such their solubility is controlled by the climatic

* Author to whom correspondence should be addressed (r.frost@qut.edu.au)

conditions in particular the temperature. The minerals can precipitate in the day time as the solution evaporates and redissolves at night when the temperature is lower. Such phenomena result in very complex mineral systems which involve jarosites and other sulphates for example iron(II)sulphates and potassium sulphate.

In many studies the assumption is made that synthetic jarosites are identical and behave the same as the natural jarosites¹⁶. Whilst some powder XRD studies can be used to study jarosites such studies are of limited value as the jarosite compounds may be poorly diffracting and the XRD pattern will be dominated by the highly crystalline materials such as potassium sulphate which is present. Vibrational spectroscopy allows a better method for the study of these minerals. Infrared spectroscopy has been used to study jarosite minerals but failed to detect cationic differences in the jarosite structures¹⁷⁻²². Raman spectroscopy has been used to study jarosites but some previous studies failed to study the complete spectra^{18,19,23}. Further the lack of crystallinity of the synthetic samples studied may have made the collection of Raman spectral data difficult. Most studies have involved the use of synthetic jarosites¹⁶. In this work, as part of our studies of secondary mineral formation, we report the comparison of the Raman spectra of natural and synthetic K and Na jarosites.

Experimental

Minerals

K-Jarosite originated from Kanmantoo, Mt Lofty Ranges, South Australia and the Na-jarosite (natrojarosite) from Londonderry, Western Australia. Synthetic jarosites were prepared. K-jarosite was synthesised as follows: A solution of 0.15M $\text{Fe}_2(\text{SO}_4)_3 \cdot 9\text{H}_2\text{O}$ and 0.5M $\text{Fe}(\text{NO}_3)_3 \cdot 9\text{H}_2\text{O}$ to this a solution of 2M KOH (Fe:KOH, 2.25) was added with vigorous stirring. The solution was kept at 95°C through out the addition then aged for a further 4 hours at this temperature. Na-Jarosite was synthesised as follows: A solution of 0.15M $\text{Fe}_2(\text{SO}_4)_3 \cdot 9\text{H}_2\text{O}$ and 0.5M $\text{Fe}(\text{NO}_3)_3 \cdot 9\text{H}_2\text{O}$ to this a solution of 1M NaOH/2.12M $\text{Na}(\text{NO}_3)_3$ (Fe:Na:OH, 1:1.12:2.35) was added with vigorous stirring. The solution was kept at 80°C through out the addition then aged for a further 24 hours at this temperature. The minerals were analysed by X-ray diffraction for phase purity and by electron probe using energy dispersive techniques for quantitative chemical composition.

Raman spectroscopy

The crystals of the particular jarosite were placed and oriented on the stage of an Olympus BHSM microscope, equipped with 10x and 50x objectives and part of a Renishaw 1000 Raman microscope system, which also includes a monochromator, a filter system and a Charge Coupled Device (CCD). Raman spectra were excited by a HeNe laser (633 nm) at a resolution of 2 cm^{-1} in the range between 100 and 4000 cm^{-1} . Repeated acquisition using the highest magnification was accumulated to improve the signal to noise ratio. Spectra were calibrated using the 520.5 cm^{-1} line of a silicon wafer. In order to ensure that the correct spectra are obtained, the incident excitation radiation was scrambled. Previous studies by the authors provide more details of the experimental technique²⁴⁻²⁷. Spectra at elevated temperatures were

obtained using a Linkam thermal stage (Scientific Instruments Ltd, Waterfield, Surrey, England).

Infrared spectra were obtained using a Nicolet Nexus 870 FTIR spectrometer with a smart endurance single bounce diamond ATR cell. Spectra over the 4000–525 cm^{-1} range were obtained by the co-addition of 64 scans with a resolution of 4 cm^{-1} and a mirror velocity of 0.6329 cm/s . Spectral manipulation such as baseline adjustment, smoothing and normalisation was performed using the GRAMS® software package (Galactic Industries Corporation, Salem, NH, USA).

Results and discussion

Sulphates as with other oxyanions lend themselves to analysis by Raman spectroscopy²⁷. In aqueous systems, the sulphate anion is of T_d symmetry and is characterised by Raman bands at 981 cm^{-1} (ν_1), 451 cm^{-1} (ν_2), 1104 cm^{-1} (ν_3) and 613 cm^{-1} (ν_4). Reduction in symmetry in the crystal structure of sulphates such as jarosites will cause the splitting of these vibrational modes. For jarosites the space group is C_5^3 and six sulphate fundamentals should be observed.

The Raman spectra of the synthetic and natural K-jarosites and Na-jarosites in the 2700 to 3800 cm^{-1} region are shown in Figures 1 and 2 and the results of the Raman spectral analysis of the reported in Tables 1 and 2. Remarkable differences are observed in the OH stretching region between the natural and synthetic jarosites. The synthetic jarosite spectrum at both 298 and 77 K consist of broad overlapping bands. In the 298 K spectrum two bands are observed at 3411 and 3292 cm^{-1} with band widths of 134.6 and 354.2 cm^{-1} . In comparison the natural jarosite shows three principal bands at 3426.1, 3388.5 and 3357.9 cm^{-1} with band widths of 78.6, 38.6 and 25.1 cm^{-1} . The natural jarosite Raman spectrum at 77 K shows good band separation with significant band narrowing. Four bands are observed at 3411, 3390, 3384 and 3348 cm^{-1} with band widths of 44.8, 16.0, 11.3 and 13.7 cm^{-1} . The difference in the spectra between the synthetic and natural K-jarosites is attributed to the differences in the hydrogen bonding and the arrangement of the hydroxyl units in the crystal structure. By using a Libowitzky type formula calculations of the hydrogen bond distances can be made using the position of the hydroxyl stretching vibrations. Calculations for the synthetic K-jarosite provides hydrogen bond distances of 2.74 and 2.80 Å. The hydrogen bond distances for the natural K-jarosite are 2.77, 2.79 and 2.81 Å. Thus the hydrogen bond distances are similar. However it is the distribution of the hydrogen bonds that is important. Variation in the hydrogen bond distance for the 3411 cm^{-1} band is between 2.760 and 2.867 Å. The variation for the 3292 cm^{-1} band is between 2.678 and 2.857 Å. In contrast the variation in hydrogen bond distance for the 3388 cm^{-1} band of the natural K-jarosite is between 2.778 and 2.796 Å and for the 3357 cm^{-1} band is between 2.764 and 2.778 Å. The variation of the hydrogen bond distances is even less at 77 K. Thus the major difference between the natural and synthetic K-jarosites is no the hydrogen bond distance but the variation in this distance.

A similar set of results exists for the OH stretching region of the Na-jarosites (Figure 2). The Raman spectrum of the synthetic Na-jarosite at 77 K shows two partially resolved bands at 3397.6 and 3350.6 cm^{-1} with bandwidths of 70.7 and 25.7

cm^{-1} . That of the natural jarosite at 77 K shows a sharp band at 3408.8 cm^{-1} with bandwidth of 10.9 cm^{-1} with a second band at 3376 cm^{-1} with bandwidth of 12.9 cm^{-1} . The widths of the hydroxyl stretching bands are also reflected in the infrared spectra which also show bands due to adsorbed water. The latter is not observed in the Raman spectra as water is a very poor Raman scatterer. The Raman spectra of the natural jarosites show that the OH units are not identical in the structure. The width of the Raman bands of the OH units serve to show that natural jarosites are highly crystalline compared with the synthetic jarosites.

The Raman spectra of the 900 to 1300 cm^{-1} region of synthetic and natural K-jarosites and Na-jarosites are shown in **Figures 3 and 4**. Three bands are observed at 1009.8 , 1011.9 and 1026.3 cm^{-1} with bandwidths of 4.4 , 6.1 and 11.5 cm^{-1} . These bands are assigned to the $(\nu_1) \text{SO}_4^{2-}$ symmetric stretching mode. The observation of more than one band may be accounted for by the non-equivalence of the SO_4^{2-} units. In the 77 K spectrum of the natural jarosite the two most intense bands are observed at 1012.8 and 1032.3 cm^{-1} with band widths of 4.7 and 7.4 cm^{-1} . In the spectra of the synthetic jarosite the most intense band is observed at 1006.5 cm^{-1} with other bands at 1036.9 and 1050.6 cm^{-1} . The latter band is due to traces of nitrate from the preparation route. A previous study by Sasaki et al. reported the band as a single band at 1006.7 cm^{-1} for a synthetic K-jarosite ²³ which is in excellent agreement with this study. However the position of the band differs from that of the natural jarosite. The difference between the spectra of the natural and synthetic jarosites for the SO_4^{2-} symmetric stretching band lies with the width of the bands. The SO_4^{2-} bandwidth for the natural jarosite indicates the mineral to be more highly crystalline than the synthetic jarosite. The Raman spectrum of natural Na-jarosite shows an intense band at 1007.0 cm^{-1} with a bandwidth of 5.1 cm^{-1} . A second band may be curve resolved at 1010.7 cm^{-1} . In the 77 K spectrum, the band is observed at 1007.6 cm^{-1} with a bandwidth of 4.9 cm^{-1} . The second band is now found at 1017.7 cm^{-1} and is partially band separated. For the synthetic jarosite the band is observed at 1011.3 cm^{-1} with a bandwidth of 8.3 cm^{-1} . A second band is observed at 1026.2 cm^{-1} . The study by Sasaki et al. showed a jarosite symmetric stretching band at 1012.1 cm^{-1} ²³. Thus just as for the Raman bands for the hydroxyl units, so also for the sulphate units. The difference between the synthetic and natural jarosites is in the bandwidth rather than the position of the band.

The Raman spectrum of the K-jarosite at 298 shows two bands at 1111.0 and 1153.1 cm^{-1} . These bands are attributed to the ν_3 antisymmetric stretching mode of the sulphate units. Two bands were reported by Sasaki et al at 1102.6 and 1153.3 cm^{-1} for a synthetic K-jarosite which is in excellent agreement with these values. The two bands are observed at 1116.3 and 1152.6 cm^{-1} in the 77 K spectrum of K jarosite. For the synthetic K-jarosite the two bands are found at 1103.8 and 1157.5 cm^{-1} in the 298 K spectrum and at 1107.2 and 1157.9 cm^{-1} in the 77 K spectrum. For natural Na-jarosite the two antisymmetric stretching bands are observed at 1102.8 and 1153.5 cm^{-1} in the 298 K spectrum and at 1105.8 and 1153.7 cm^{-1} in the 77 K spectrum. The synthetic Na jarosite has Raman bands at 1110.2 and 1158.4 cm^{-1} . These results show that there are subtle differences in band positions between the natural and synthetic K and Na-jarosites.

The Raman spectra of the low wavenumber region for K and Na jarosites are shown in **Figures 5 and 6**. K-jarosite shows two overlapping bands at 443.7 and 452.8 cm^{-1} with bandwidths of 12.0 and 10.7 cm^{-1} and are assigned to the ν_2 bending mode. The observation of two bands is simply due to symmetry lowering. The values differ considerably from that published for synthetic K-jarosite²³. Sasaki et al. assigned the most intense band at 434.5 cm^{-1} to FeO stretching vibrations. Such an assignment is unlikely. The band is attributed to the ν_2 bending mode. Two bands are found at 354 to 365 cm^{-1} and at around 300 cm^{-1} . These bands are more likely due to FeO vibrations. These two bands are found at 446.6 and 453.9 cm^{-1} in the 77 K spectrum. For the synthetic K-jarosite the two bands are found at 433.1 and 454.3 cm^{-1} and are significantly broader. Two bands are identified for natural Na-jarosite at 434.6 and 453.9 cm^{-1} with bandwidths of 9.0 and 7.7 cm^{-1} . These bands are observed at 436.7 and 454.3 cm^{-1} in the 77 K spectrum. For the synthetic Na-jarosite the bands are found at 439.7 and 453.3 cm^{-1} . The band widths are 18.0 and 14.0 cm^{-1} . Again as for the hydroxyl stretching and the sulphate stretching region the bands for the synthetic K and Na jarosites are considerably broader than the natural K and Na jarosites.

The spectra of the K and Na jarosites in the low wavenumber region show bands at around 575, 625 and 641 cm^{-1} . The latter two bands are ascribed to the ν_4 bending modes of the sulphate and the first band may be assigned to a FeOH deformation mode. The two bands at 641.7 and 624.9 cm^{-1} in the 298 K spectrum for natural K-jarosite shift to 645 and 625.6 cm^{-1} in the 77 K spectrum. These bands are not well defined for the synthetic jarosite. The predominant band is at 623.4 cm^{-1} with a broad shoulder at 649.8 cm^{-1} . The band at 565.9 cm^{-1} appears to split into two bands at 575.5 and 566.6 cm^{-1} in the 77 K spectrum for the synthetic Na-jarosite. In the spectra of the low wavenumber region of the K and Na jarosites two bands are found at around 366 and 299 cm^{-1} . One probable assignment of the bands is to FeO stretching vibrations. An intense band is also found at around 230 cm^{-1} . It is attributed to FeO vibration. These bands are considerably broader for the synthetic jarosites as compared to the natural minerals.

Conclusions

The jarosite mineral group can be characterised by their Raman spectra. In this work a comparison has been made between natural and synthetic K and Na-jarosites. However the spectra of the synthetic minerals may not necessarily be the same as the natural minerals.

There is a fundamental assumption about synthetic minerals being the same as the natural minerals which in fact may not be correct. With respect to jarosites a number of points can be made:

(a) Minerals such as jarosites usually are formed at different localities under different conditions. Crystal structures of thus formed minerals may vary.

(b) Synthetic analogues are synthesized under laboratory conditions which are mostly different from those in nature. Their crystal structures may be identical but their molecular structure may differ from natural phases.

(c) In the case of hydroxylated minerals such as jarosites, for phases formed under different conditions (various localities, different laboratories and procedures) the hydrogen-bonding network may significantly vary.

(d) X-ray powder pattern identity does not mean that the same minerals from various localities and their synthetic analogues prepared by various methods and procedures have identical crystal structures. Raman spectroscopy shows the jarosite minerals may differ at the molecular level.

(e) Hydrogen-bonding network may play an important role in the origin/formation of minerals and their synthetic analogues. This may be one of the big differences between the highly crystalline natural jarosites and the synthetic analogues.

(f) Phases of the same composition formed under normal temperature and under hydrothermal conditions need not be identical, may differ e.g. in bond lengths.

(g) Hydrated and anhydrous systems (minerals formed from solutions such as jarosites) may vary in comparison with anhydrous systems connected with reactions/processes in solid state under different/various temperatures.

(h) It is obvious that the conditions of mineral origin in nature cannot be identical with those in a laboratory and probably neither comparable.

In conclusion, solutions of these problems may be not possible with X-ray powder or single crystal analysis, however, the careful study using Raman spectroscopy perhaps complimented by infrared spectroscopy can help solve these problems.

References

1. Madden, MEE, Bodnar, RJ, Rimstidt, JD. *Nature* 2004; **431**: 821.
2. Vaniman, DT, Bish, DL, Chipera, SJ, Fialips, CI, William Carey, J, Feldman, WC. *Nature (London, United Kingdom)* 2004; **431**: 663.
3. Bibring, J-P, Langevin, Y, Poulet, F, Gendrin, A, Gondet, B, Berthe, M, Soufflot, A, Drossart, P, Combes, M, Bellucci, G, Moroz, V, Mangold, N, Schmitt, B. *Nature (London, United Kingdom)* 2004; **428**: 627.
4. Hynek, BM. *Nature (London, United Kingdom)* 2004; **431**: 156.
5. Swamy, MSR, Prasad, TP, Sant, BR. *Journal of Thermal Analysis* 1979; **16**: 471.
6. Swamy, MSR, Prasad, TP, Sant, BR. *Journal of Thermal Analysis* 1979; **15**: 307.
7. Bhattacharyya, S, Bhattacharyya, SN. *Journal of Chemical and Engineering Data* 1979; **24**: 93.
8. Swami, MSR, Prasad, TP. *Journal of Thermal Analysis* 1980; **19**: 297.
9. Swamy, MSR, Prasad, TP. *Journal of Thermal Analysis* 1981; **20**: 107.
10. Banerjee, AC, Sood, S. *Therm. Anal., Proc. Int. Conf., 7th* 1982; **1**: 769.
11. Buckby, T, Black, S, Coleman, ML, Hodson, ME. *Mineralogical Magazine* 2003; **67**: 263.
12. Williams, PA *Oxide Zone Geochemistry*; Ellis Horwood Ltd, Chichester, West Sussex, England, 1990.
13. Drouet, C, Baron, D, Navrotsky, A. *American Mineralogist* 2003; **88**: 1949.
14. Paktunc, D, Dutrizac, JE. *Canadian Mineralogist* 2003; **41**: 905.
15. Stoffregen, RE, Alpers, CN, Jambor, JL. *Reviews in Mineralogy & Geochemistry* 2000; **40**: 453.
16. Drouet, C, Navrotsky, A. *Geochimica et Cosmochimica Acta* 2003; **67**: 2063.
17. Adler, HH, Kerr, PF. *American Mineralogist* 1965; **50**: 132.
18. Serna, CJ, Parada Cortina, C, Garcia Ramos, JV. *Spectrochimica Acta, Part A: Molecular and Biomolecular Spectroscopy* 1986; **42A**: 729.
19. Sasaki, K. *Canadian Mineralogist* 1997; **35**: 999.
20. Omori, K, Kerr, PF. *Geological Society of America Bulletin* 1963; **74**: 709.
21. Hunt, GR. *Geophysics* 1979; **44**: 1974.
22. Arkhipenko, DK, Devyatkina, ET, Pal'chik, NA. *Kristalloghimiya i Rentgenogr. Mineralov, L.* 1987: 138.
23. Sasaki, K, Tanaike, O, Konno, H. *Canadian Mineralogist* 1998; **36**: 1225.
24. Frost, RL. *Analytica Chimica Acta* 2004; **517**: 207.
25. Frost, RL, Kloprogge, JT, Martens, WN. *Journal of Raman Spectroscopy* 2004; **35**: 28.
26. Frost, RL, Weier, ML. *Journal of Raman Spectroscopy* 2004; **35**: 299.
27. Frost, RL, Williams, PA, Martens, W, Leverett, P, Kloprogge, JT. *American Mineralogist* 2004; **89**: 1130.

List of Figures

Figure 1 Raman spectra of the hydroxyl stretching region of natural and synthetic K-jarosite at 298 and 77 K.

Figure 2 Raman spectra of the hydroxyl stretching region of natural and synthetic Na-jarosite at 298 and 77 K.

Figure 3 Raman spectra of the 900-1300 cm^{-1} region of natural and synthetic K-jarosite at 298 and 77 K.

Figure 4 Raman spectra of the 900-1300 cm^{-1} region of natural and synthetic Na-jarosite at 298 and 77 K.

Figure 5 Raman spectra of the 100-800 cm^{-1} region of natural and synthetic K-jarosite at 298 and 77 K.

Figure 6 Raman spectra of the 100-800 cm^{-1} region of natural and synthetic Na-jarosite at 298 and 77 K.

List of Tables

Table 1 Results of the Raman spectral analysis of natural and synthetic K-jarosite.

Table 2 Results of the Raman spectral analysis of natural and synthetic Na-jarosite

Table 1 Results of the Raman spectrum of synthetic and natural jarosite

g19611 298K			g19611 77K			synthetic 298K			synthetic 77K		
Centre	FWHM	%	Centre	FWHM	%	Centre	FWHM	%	Centre	FWHM	%
3573.2	68.5	0.6	3578.5	40.5	0.3						
3511.1	51.4	0.7	3506.5	23.6	0.2						
			3445.6	23.4	0.6						
3426.1	78.6	10.3	3411.0	44.8	16.0	3411.3	134.6	13.5	3421.0	54.9	1.8
3388.5	38.6	13.4	3390.4	16.0	2.6				3395.3	130.3	8.6
			3384.7	11.3	11.3						
3357.9	25.1	1.5	3348.3	13.7	2.4						
			3328.9	150.7	1.7						
3305.5	123.0	4.3							3308.8	357.8	16.0
3166.2	144.8	0.9				3292.7	354.2	12.9			
									3078.4	483.5	5.5
2030.5	58.6	0.3	2046.4	30.2	0.4	2945.2	280.3	2.3			
			2013.3	15.9	0.1	2010.3	69.6	0.2			
			1954.8	10.3	0.1						
1695.9	51.6	0.5	1708.9	64.0	1.9	1689.8	60.7	0.3	1700.1	54.2	0.2
			1585.8	114.3	0.5	1625.8	93.1	0.5	1630.9	78.7	0.4
						1447.5	57.5	0.2	1438.1	66.1	0.3
1239.5	52.3	0.2									
1183.6	46.1	0.4							1182.6	82.6	3.7
						1167.5	93.6	5.6			
1153.1	22.3	7.0	1152.6	19.1	9.0	1159.3	19.0	0.4	1157.9	20.9	0.7
1128.6	25.5	0.6	1134.0	10.4	0.2						
1111.0	12.7	13.9	1116.3	7.2	12.7				1107.2	30.7	12.7
						1103.8	28.0	12.4	1107.0	7.9	0.2

1080.2	31.9	0.8	1091.9	17.3	0.4				1092.1	4.6	0.1
			1064.2	43.5	0.5	1050.6	8.1	0.3	1051.2	10.5	1.0
1039.3	30.7	0.9	1032.3	7.4	1.8	1036.9	17.9	0.5	1036.1	13.1	0.2
1026.3	11.5	0.9	1018.3	5.3	0.7	1022.8	68.2	6.0			
1011.9	6.1	4.9	1012.8	4.7	6.2				1013.2	6.3	0.2
									1011.3	50.6	7.7
1009.8	4.4	1.1	1007.1	3.6	0.3	1006.5	10.0	6.3	1007.0	7.3	2.8
998.0	22.4	0.2	1000.2	14.5	0.2	992.0	5.3	0.1	994.4	5.9	0.1
944.2	89.8	0.4									
879.7	34.5	0.1									
						718.2	66.0	1.2	723.7	43.0	0.9
649.4	20.5	1.4	655.5	10.4	2.0	644.5	17.1	0.3	645.7	9.1	0.1
632.7	8.2	0.2	625.1	5.8	3.1						
623.9	6.9	3.2	624.5	5.4	2.7	624.9	11.4	1.3	626.1	11.4	2.0
617.2	14.2	0.4									
			577.5	14.6	2.0	576.8	29.8	4.3	582.7	30.2	5.4
566.2	26.9	5.3	562.2	12.5	0.8	558.8	83.0	8.5	554.6	41.9	3.9
544.7	32.8	0.3									
472.9	72.3	0.4							469.0	15.4	0.2
452.8	10.7	2.3	453.9	9.2	3.5	454.3	18.9	2.0	455.1	12.8	2.1
443.7	12.0	10.3	446.6	6.8	6.1						
			440.1	12.8	1.6	433.1	16.6	3.7	435.4	9.0	1.3
									432.1	28.6	10.9
406.3	92.8	0.5				408.7	74.3	2.1			
									400.1	56.2	3.8
365.0	14.9	0.8	369.8	6.7	0.4	366.7	155.8	6.0	359.2	20.7	1.3
						356.5	18.0	0.9			
						316.5	21.3	0.5	322.4	24.0	1.1
296.7	14.7	1.2	298.9	9.0	1.2	299.2	18.8	1.6	300.3	16.9	1.4
289.9	72.0	1.9				253.4	43.7	1.2	266.4	23.9	0.7
244.4	25.6	0.8	242.9	7.2	0.1						
			240.2	45.9	0.6				233.8	38.9	1.1

225.9	11.3	6.1	231.3	6.5	5.9	224.4	22.9	4.3	228.0	15.3	1.4
211.3	47.0	1.0				205.6	23.6	0.4			
			188.1	8.2	0.1				162.9	7.0	0.0
165.0	11.2	0.0							142.1	7.0	0.0
140.0	5.3	0.0									

Table 2 Results of the Raman spectra of natural and synthetic Natrojarosite

g20148 298K			g20148 77K			synthetic 298K			synthetic 77K		
Centre	FWHM	%	Centre	FWHM	%	Centre	FWHM	%	Centre	FWHM	%
3530.2	29.4	0.1									
3465.7	40.2	1.4	3471.1	19.4	0.8						
			3453.3	15.5	1.2						
3433.5	77.9	10.1	3429.2	42.2	7.5						
3409.7	19.3	11.2	3408.8	10.9	19.8	3398.1	115.4	17.8	3397.6	70.7	15.5
3382.8	20.9	3.8	3376.2	12.9	2.3						
						3360.0	12.2	0.1	3350.6	25.7	1.9
3304.2	58.3	1.0									
						3281.4	322.5	8.1	3322.3	183.1	9.8
3229.4	42.7	0.1									
3167.2	40.0	0.1				2909.9	115.2	0.5			
2203.9	30.0	0.1				2028.2	89.1	0.6			
2016.5	63.4	0.4	2012.3	57.1	0.8						
2006.4	14.3	0.1									
1976.4	22.8	0.1									
1922.5	16.4	0.0	1935.2	90.3	0.8						
1693.1	47.8	0.6	1692.8	54.2	1.7	1698.4	45.5	0.1			
						1655.7	136.6	0.6			
									1595.2	123.9	13.3
									1479.0	90.4	2.2
									1356.5	132.8	7.3
						1248.3	11.3	0.0			
						1211.4	143.1	1.0			
1161.8	25.8	0.5				1158.4	35.4	3.9			
1153.5	14.6	6.9	1153.7	11.5	7.5	1155.4	16.0	0.6	1156.6	27.7	3.2

1114.5	42.1	1.3				1123.0	16.9	0.9	1115.3	18.2	14.2
1111.5	135.5	2.9				1110.2	19.2	14.1			
1102.8	10.3	8.5	1105.8	8.0	13.6						
1080.4	14.8	0.2				1091.6	36.7	1.0	1075.5	31.9	0.9
						1051.0	20.4	0.7	1040.4	29.6	1.9
						1035.5	18.2	1.3	1029.1	14.5	1.2
						1026.2	8.1	0.4			
1010.7	12.0	3.7	1017.7	8.9	2.1	1011.3	8.3	8.5	1012.6	6.9	5.8
1007.0	5.1	5.6	1007.6	4.9	7.2				1002.2	14.8	2.0
			994.8	12.1	0.2	995.9	18.2	0.7			
			943.2	52.6	0.6						
						700.4	87.5	0.4	819.2	16.7	0.8
641.7	13.5	0.7	645.0	7.2	1.7	649.8	21.0	0.3	652.1	18.2	0.4
624.9	5.8	4.3	625.6	5.4	5.0	623.4	9.5	3.0	624.3	8.1	1.7
614.6	12.4	0.2									
575.7	17.4	2.2	581.3	11.8	2.7				575.5	45.5	3.6
						565.9	42.2	7.5	566.6	23.6	1.8
550.2	20.1	1.5	554.9	9.3	0.5	563.2	13.9	0.3			
460.4	31.7	1.1				467.4	19.4	0.2			
453.9	7.7	3.3	454.3	7.7	1.9	453.3	14.0	3.5	454.6	9.8	2.5
443.3	9.8	1.8	444.9	5.8	1.1				442.4	13.4	2.9
434.6	9.0	9.4	436.7	6.4	9.3	439.7	18.0	8.9			
426.2	54.6	0.9	425.7	11.2	0.5						
						397.0	64.6	5.6	393.3	37.5	2.2
354.8	12.0	1.8	357.1	7.0	0.7	362.7	17.4	0.8	366.0	10.7	0.6
322.7	19.1	0.6									
300.6	10.1	2.3	302.1	7.0	2.0	296.4	23.9	2.0	298.2	16.6	2.3
288.0	52.0	1.2				282.1	64.0	1.1			
			237.8	12.1	0.6	248.6	26.9	0.8			
227.6	20.9	2.1	227.6	6.3	7.7	225.6	17.9	3.9	230.6	12.8	1.7
223.8	8.4	7.5									
210.4	9.6	0.4	210.0	4.3	0.1	205.3	27.8	0.4			

194.9	36.9	0.1	184.6	6.3	0.1	183.0	10.3	0.0	183.7	7.5	0.2
139.9	4.4	0.0				139.4	6.8	0.1			

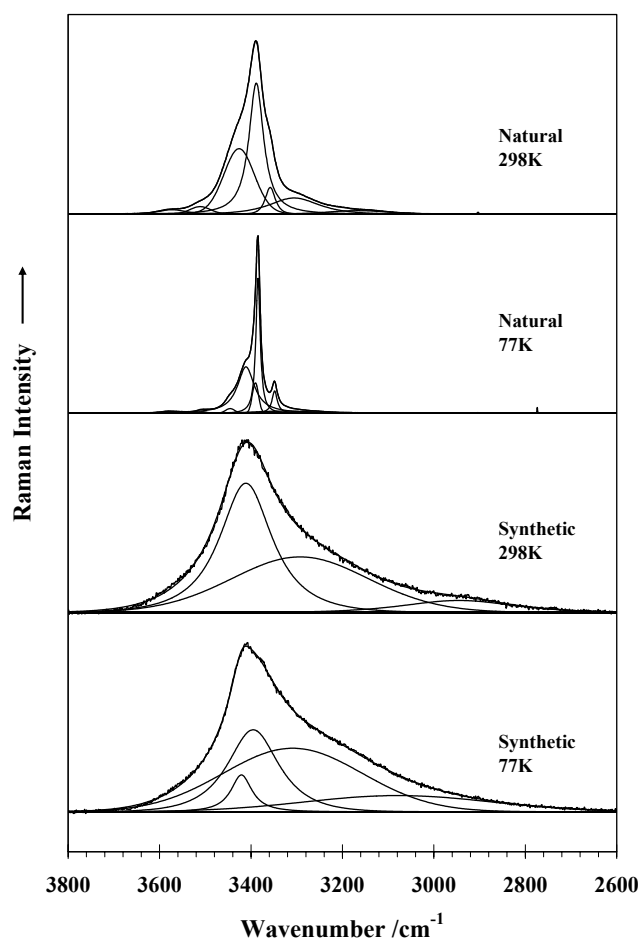


Figure 1

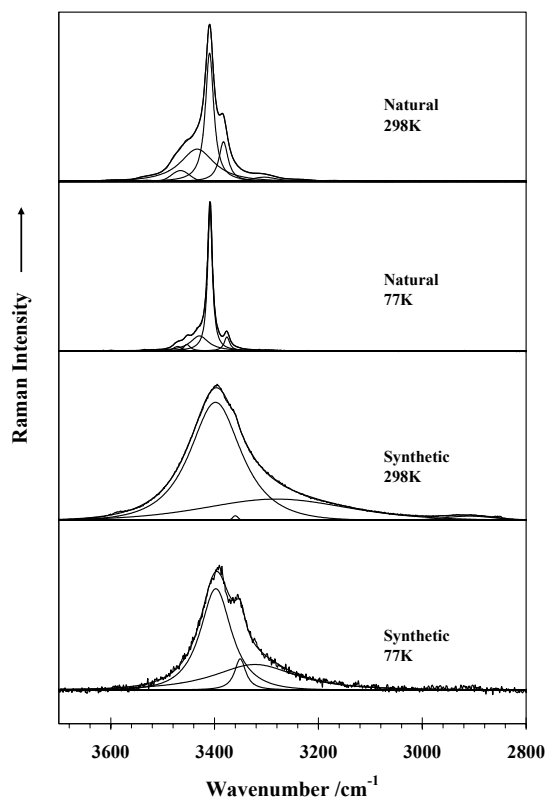


Figure 2

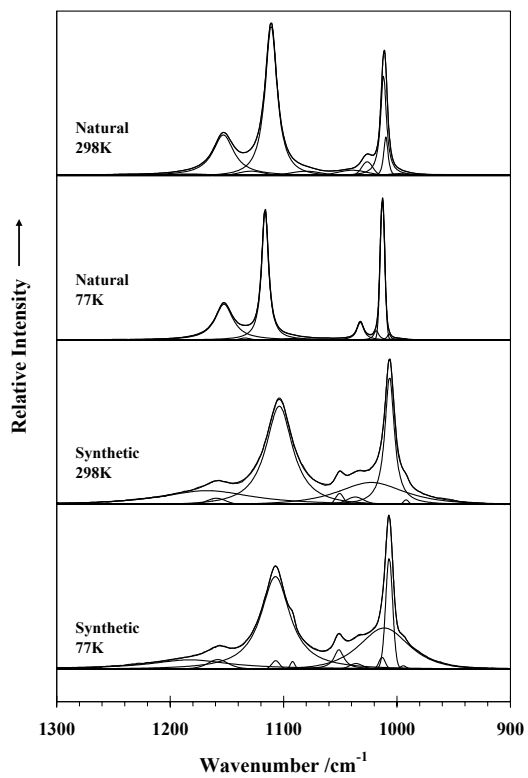


Figure 3

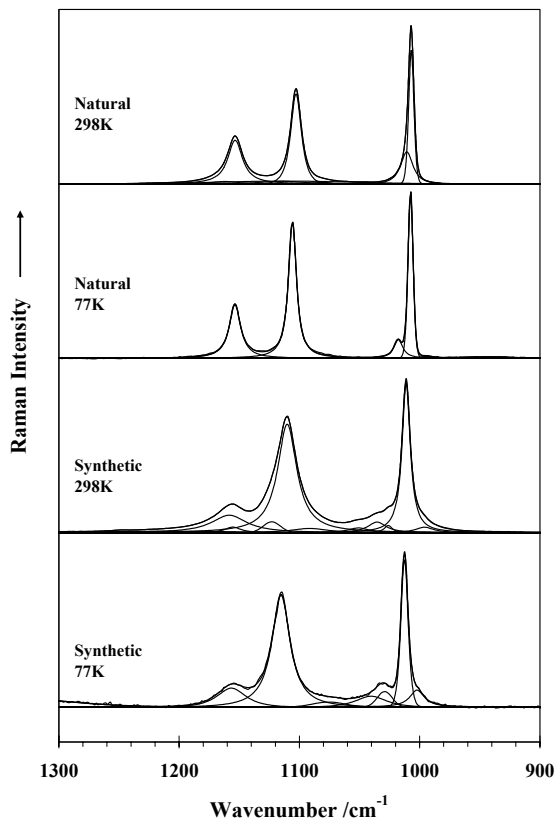


Figure 4

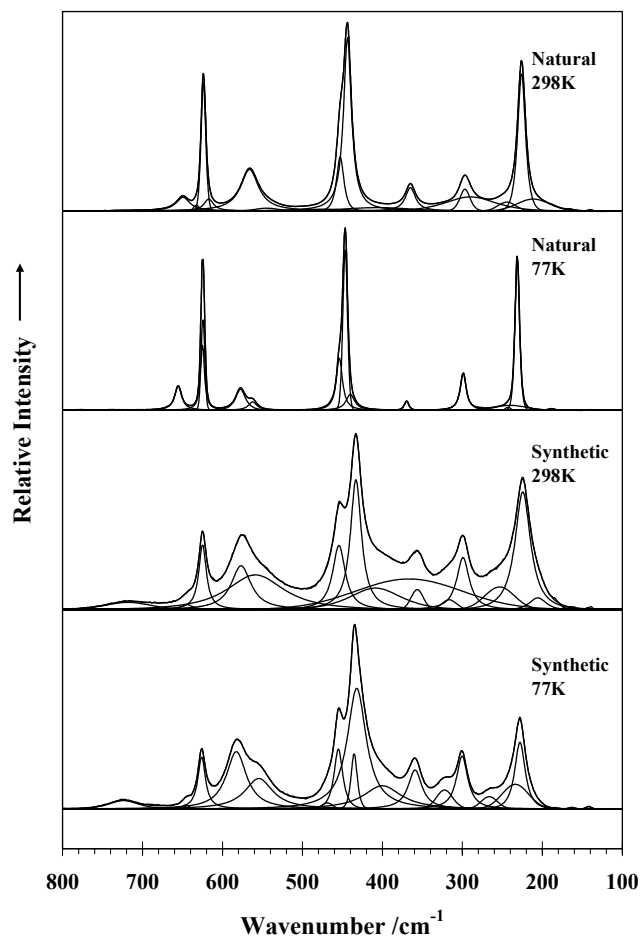


Figure 5

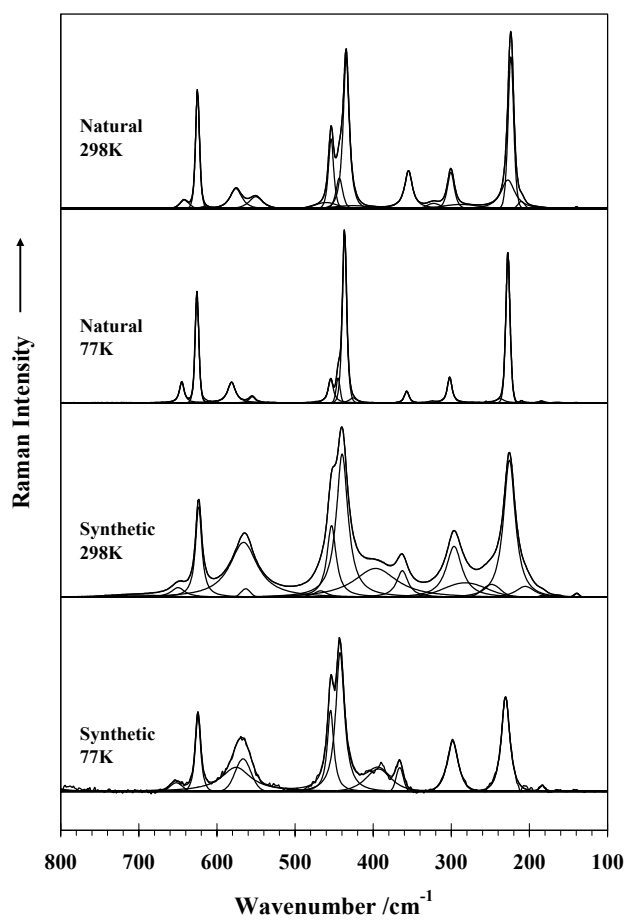


Figure 6

